



Universiteit
Leiden
The Netherlands

The origins of friction and the growth of graphene, investigated at the atomic scale

Baarle, D.W. van

Citation

Baarle, D. W. van. (2016, November 29). *The origins of friction and the growth of graphene, investigated at the atomic scale. Casimir PhD Series*. Retrieved from <https://hdl.handle.net/1887/44539>

Version: Not Applicable (or Unknown)

License: [Licence agreement concerning inclusion of doctoral thesis in the Institutional Repository of the University of Leiden](#)

Downloaded from: <https://hdl.handle.net/1887/44539>

Note: To cite this publication please use the final published version (if applicable).

Cover Page



Universiteit Leiden



The handle <http://hdl.handle.net/1887/44539> holds various files of this Leiden University dissertation.

Author: Baarle, D.W. van

Title: The origins of friction and the growth of graphene, investigated at the atomic scale

Issue Date: 2016-11-29

Chapter 10

High-temperature behaviour of graphene-covered iridium

In the preceding chapters, the nucleation and growth of graphene on the (111) surface of iridium was studied. The results have provided us with detailed insight in graphene synthesis on this substrate. In the present chapter, we continue by focussing on the behaviour of the iridium underneath the graphene at elevated temperatures. We pay special attention to the terrace edges of the iridium surface by, in the first place, looking at the growth of graphene over iridium steps. Second, we focus on the behaviour of iridium steps that are completely covered by graphene. The observations show a dominant role of the moiré pattern that is present in the graphene-iridium system. Third, small fluctuations of the iridium steps were followed. Our findings show that iridium is very mobile underneath the graphene. The iridium steps serve as channels for the transportation of iridium atoms underneath the graphene overlayer.

10.1 Graphene growth over iridium steps

The cleaned Ir(111) substrate was first pre-exposed to 0.5L ethylene at room temperature. Then, the substrate was heated up to a temperature of 1064K. At this temperature the STM imaging was started and one graphene island was kept in view. The system was exposed to a partial pressure of 2×10^{-9} mbar of ethylene while the scanning was continued.

Part of the movie of a growing graphene island on the Ir(111) surface is shown in Figure 10.1, the original movie can be found in the electronic Supplementary Material, Movie 3. In the image sequence shown here, we zoomed in on that part of the island that was growing over an iridium step.

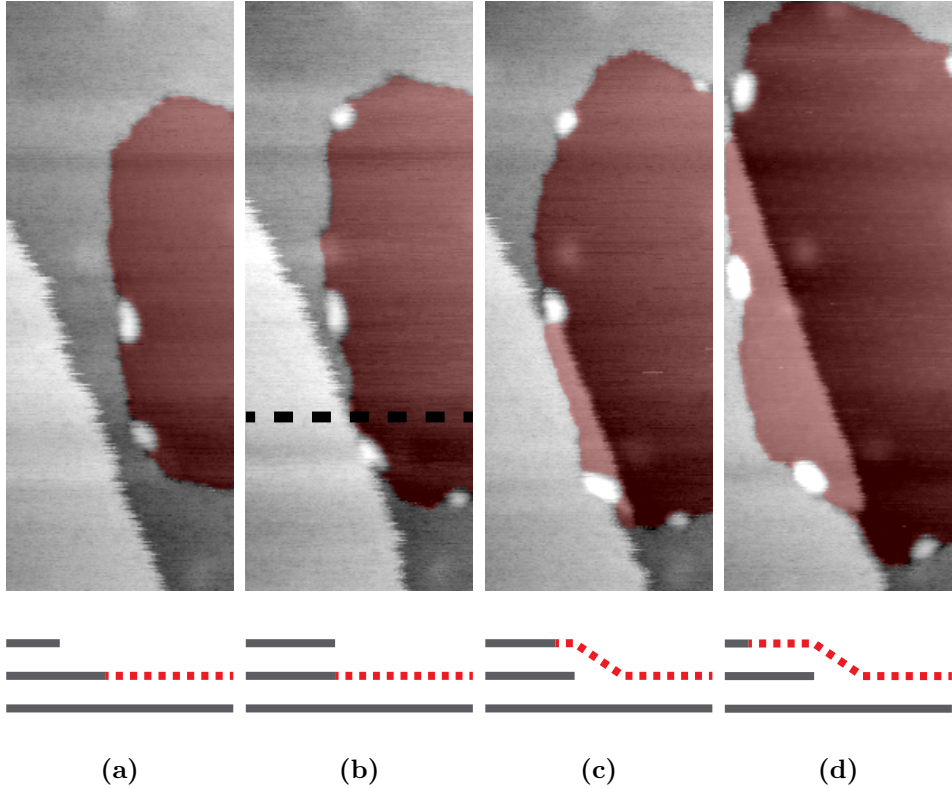


Figure 10.1: Four STM frames from an image sequence (frames 64, 68, 73 and 86) showing the growth of a graphene island on top of Ir(111), followed by STM. The images were recorded at a temperature of 1064 K, while the surface was exposed to an ethylene partial pressure of 2×10^{-9} mbar. Frames (b), (c) and (d) were recorded at times of 62, 155 and 553 sec, relative to frame (a). The red colour highlights the graphene island. For clarity a schematical cross section of the imaged surface is shown below each image. The place where the cross section is taken, is indicated by the dashed line in panel (b). Image size $33 \times 87 \text{ nm}^2$, z-scale 0.30 nm, sample voltage 2.2 V, tunnelling current 0.1 nA.

For clarity, the graphene island is highlighted with a red colour. Based on the full-sized STM images (which can be found in Movie 3), we can state that in this image the graphene is growing inside an iridium terrace. A schematic surface cross section is shown below each of the STM images in Figure 10.1. What the image sequence in Figure 10.1 shows, is that the growth of the graphene proceeds into the iridium terraces by the expulsion of iridium edge atoms. At the same time, the iridium edge underneath the graphene island advances, which indicates that a net transport of atoms from the graphene-iridium interface to other areas on the iridium surface is taking place. The latter observation will be discussed in more detail in Section 10.2.

Here, we first focus on the growth of the graphene over the iridium step. In the specific case that is presented here, graphene is growing ‘upwards’, i.e. graphene climbs on top of the iridium terrace that it was originally level with (see transition from (b) to (c) in Figure 10.1). The process of graphene growing of steps has been reported numerous times in the literature, but in most cases, the growth of the graphene islands over the surface steps is ‘downhill’[83, 86–89]. Here, we observe the opposite direction of growth: from a lower iridium terrace to a higher one, ‘uphill’.

In addition to the observation of graphene over-growing iridium in the ‘uphill’ direction, also the timing of the transition to the next iridium terrace is special. As Figure 10.1 illustrates, it is precisely when the graphene has pushed the iridium terrace edge backward so far that it runs against the next step on the iridium surface (panel (b)), that the graphene continues by growing upwards and ‘invading’ the next iridium terrace level. Apparently, the energy required to deform a double-height step on the iridium exceeds the energy investment required for the graphene to cross the step and the chemical potential of the carbon that is provided by the low pressure of ethylene is sufficient for the latter energy investment.

The growth behaviour of graphene that is presented here, is observed systematically. At this stage, we have not investigated the influence of temperature and pressure on the various growth mechanisms of graphene on iridium. Our findings show that already at a relatively low growth temperature of 1064 K graphene can grow over iridium steps. Apparently, the iridium steps are not limiting the sizes of the graphene islands, which would otherwise have been a concern for large-scale graphene production.

One might wonder about the presence of several ‘particles’ that show up as very high in the images of Figure 10.1. In our experiments, these particles appeared during the growth of graphene, only at places where graphene was growing inside the iridium terrace. The height of these par-

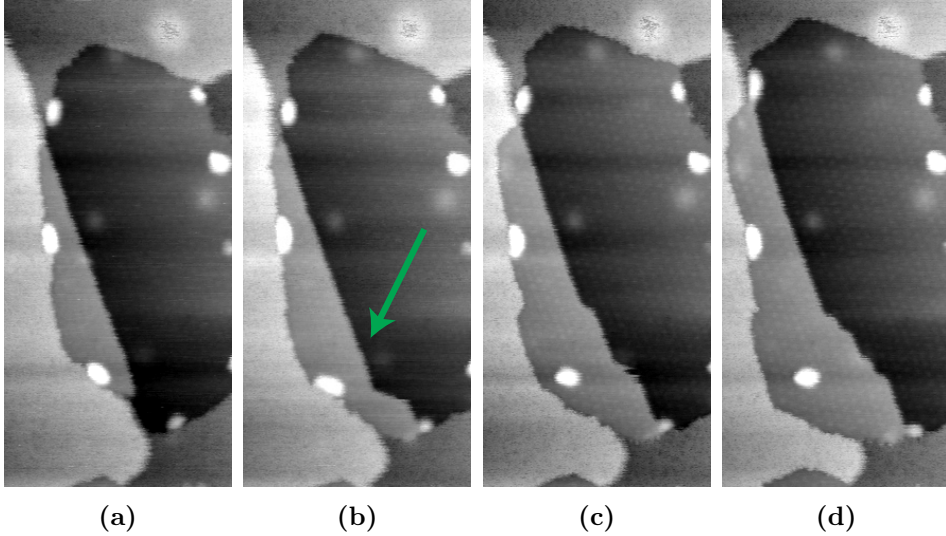


Figure 10.2: Four frames from the same STM sequence as in Figure 10.1 (frames 86, 89, 92 and 96) showing the iridium step mobility underneath graphene. The fluctuating step is indicated by the green arrow in panel (b). The images were recorded at a temperature of 1064 K, while the surface was exposed to an ethylene partial pressure of 2×10^{-9} mbar. Frames (b), (c) and (d) were acquired at times of 91, 183 and 305 sec relative to frame (a). Image size $49 \times 105 \text{ nm}^2$, z-scale 0.30 nm, sample voltage 2.2 V, tunnelling current 0.1 nA.

ticles is not identical, but they exhibit values comparable to the height (or sometimes twice the height) of an iridium terrace. As long as those particles are situated at a boundary between equally levelled graphene and iridium surfaces, they are mobile, can grow, shrink, merge and disappear. Also, they typically move along with the moving graphene-iridium boundary interface. We observed that sometimes, these particles got trapped inside the graphene, as can be seen clearly in the lower part of the images shown in Figure 10.2. From the behaviour of those particles, we assume that they mainly consist of iridium atoms. We did not observe a significant effect of the presence of those particles on the growth process of the graphene islands.

10.2 Iridium step mobility underneath graphene

The free iridium step on the left side of panel (a) in Figure 10.1 shows a frizzy appearance. This frizziness is characteristic of the rapid step fluctuations that take place on clean metal surfaces. Such fluctuations are due to transport of metal atoms either along the steps or between the steps and the neighbouring terraces [90–93]. Interestingly, when the step is overgrown by graphene, such as is the case for part of the step in panels (c) and 10.1d of Figure 10.1, the frizziness is reduced nearly to zero. In the STM images it looks as if the iridium step that is directly in contact with an edge of the growing graphene island shows no fluctuations at all. Here we concentrate further on the overgrown step in Figure 10.1, which we follow in Figure 10.2 for a total of 305 extra seconds. The images in Figure 10.2 reveal that at 1064 K the iridium underneath the graphene is still mobile: the iridium step that is indicated by the green arrow in Figure 10.2b is changing shape during the experiment. Actually, the step is advancing, which means that over time, iridium is being added to that area of the step.

The images indicate, in particular panels (c) and (d) of Figure 10.2, that the step advancement is initiated from the location where the edge of the graphene island crosses the step on the iridium surface. This part of the step advances most rapidly, while other parts of the step follow with some delay. From a geometrical point of view, it is indeed to be expected that such crossing points provide the locations where iridium atoms can slip in and be incorporated under the graphene most easily. Subsequently, these atoms diffuse along the iridium step underneath the graphene overlayer, possibly with some hindrance by the graphene, until they get incorporated more permanently in the next row of iridium atoms. That even the straight sections of the buried iridium steps are not completely immobile can be seen from the modest, residual frizziness of these edges, visible in Figures 10.1 and 10.2.

Another remarkable observation is that the shape of the advancing iridium step is not straight, but contains ‘macro-kinks’ with a width corresponding to a full unit of the moiré pattern of the graphene overlayer. The movement of these macro-kinks results in the advancement of the buried step. A zoom-in of a location at the step at which multiple macro-kinks are present, is shown in Figure 10.3. In this figure, the contrast has been increased in order to emphasise the relation of the macro-kinks to the moiré pattern. From the zoom-in, we can conclude that the size of each macro-kink is precisely the size of the moiré lattice parameter.

There are two further observations to be taken from Figure 10.3. First, the buried iridium step still exhibits fluctuations in its position, with an

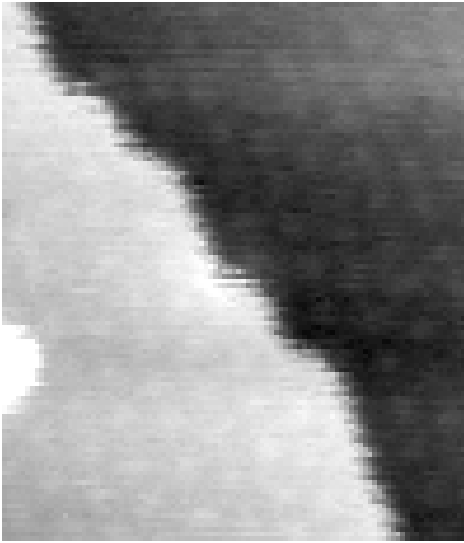


Figure 10.3: A zoom-in of the image presented in Figure 10.2d of a graphene-covered iridium step at 1064 K. The moiré units in the graphene overlayer can be distinguished, as well as the shape of the iridium step beneath the graphene that is roughly following the moiré pattern. Note, that the step also exhibits sub-moiré-unit fluctuations and that the moiré-unit-sized macro-kinks are typically spread out along the step over a distance in the order of a moiré unit. Image size $23 \times 26 \text{ nm}^2$.

amplitude well below the moiré lattice parameter (and also well below the amplitude for the free iridium step). Second, the macro-kinks are not sharp. Instead, each macro-kink is distributed along the length direction of the step over a distance in the order of a full moiré unit. The small-amplitude step fluctuations are also present in the macro-kink portions of the buried step.

The observation that the iridium step tends to follow the moiré lattice tells us that the interaction between the iridium and the graphene is significant under the experimental conditions we exposed our substrate to. Clusters of iridium atoms that are smaller than the moiré unit size appear to be unstable. From this we can conclude that approximately 9×9 iridium atoms have to be added to an existing macro-kink in order to add a new moiré sized iridium unit to that step. Of course, the 81 iridium atoms, required for the addition of a complete moiré unit, cannot be expected to arrive all at once. Intermediate configurations that are less favourable must necessarily be formed first. Our observations that nevertheless, the moiré pattern has a dominant influence on the shape of the buried iridium steps, indicates that the intermediate configurations have significantly higher formation energies. In addition, we remark that it might be that due to the continued ‘supply’ of iridium atoms to the buried step, the concentration of mobile iridium ‘adatoms’ attached to the iridium step is slowly increasing over time and at a well-defined concentration the barrier is overcome for the successful formation of an additional moiré unit to the advancing iridium macro-kink.

The advancement of a buried iridium step in units of the moiré pattern has a strong analogy with the advancement that we have encountered in Chapter 7 of the edges of growing graphene islands. Also for graphene growth, the moiré pattern has a dominating influence, forcing the graphene to grow in units of the moiré lattice. Of course, the energy differences that are at play in both cases are the same. However, an element that brings in a significant difference is the freedom of the graphene to distort significantly at its edges, which leads to the sub-moiré-unit growth ‘strategy’ that we identified for the advancing graphene edges in Chapter 7, for which we find no counterpart here.

One of the remaining questions concerns the origin of the iridium atoms that contribute to the advancement of the steps underneath the graphene. Where do these iridium atoms come from? Why is there net transport of iridium atoms to the buried steps? The answer to these questions is related to the growth of graphene islands into iridium terraces, as observed in Figures 10.1 and 10.2. As we have recognized already, this growth proceeds

by the combination of the advancement of graphene edges and the simultaneous retraction of the iridium steps that they are in direct contact with. This results in a supply of expelled iridium atoms that only ends when the graphene layer is complete. The expelled atoms cannot leave the surface. Nor do we observe their accumulation in iridium adatom islands. Instead, these iridium atoms find their way to the buried iridium steps, which they force to advance in the progress.

10.3 Fluctuations of graphene-covered iridium steps

In the previous section, we reported the observation of mobility of the iridium steps that are covered with graphene. In order to understand the dynamics of the iridium underneath graphene, we studied the high-temperature behaviour of iridium underneath graphene in more detail. Our results are reminiscent of fluctuations of terrace edges on surfaces, recorded at much lower temperature[90–95]. However, in our study, the fluctuations do not take place on the atomic scale, but are characterized by the moiré unit cell, which contains 81 iridium atoms. Apparently, transport of hundreds of mobile iridium atoms takes place underneath the graphene overlayer. Furthermore, we present additional evidence for the nature of the fluctuation as discussed by our group before[95, 96].

10.3.1 Experimental approach

After cleaning and annealing of the iridium surface, graphene was grown by the following method: the iridium substrate was heated up to 1200 K and kept at that temperature for approximately 6000 sec. The background pressure remained below 1×10^{-9} mbar. In this manner, carbon that was remaining in the substrate from previous experiments was used as the main source for the graphene. This procedure resulted in a partial coverage of large (> 100 nm in diameter) graphene flakes. At this high temperature, the substrate was followed by the STM continuously until graphene grew into the field of view of the STM. Subsequently, the focus was set to iridium steps underneath the graphene while the temperature was kept between 1160 and 1210 K. Several scan rotations were applied to characterise the nature of the iridium step fluctuations.

As, in this particular study of fluctuations, the timing of the STM data acquisition is very relevant, we briefly discuss the applied image acquisition procedure. Figure 10.4 indicates the path of the STM tip during the acqui-

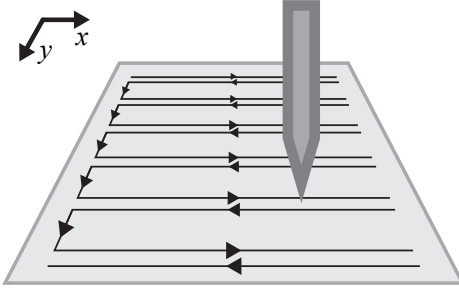


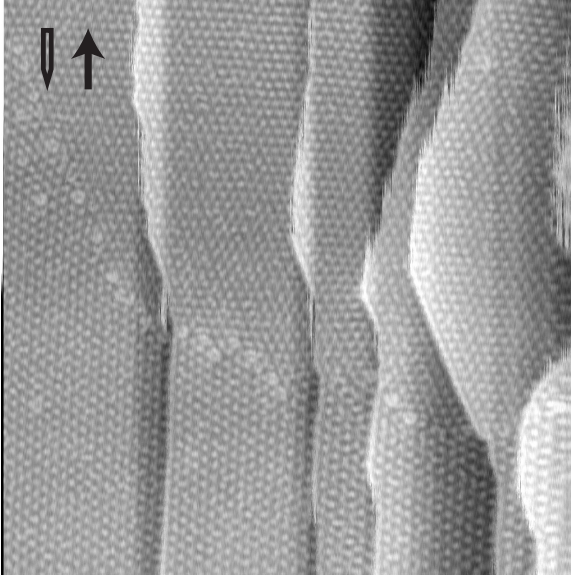
Figure 10.4: Schematics explaining how the STM-tip moves, while the STM-data is recorded. A forward and a backward trace in the x-direction are performed first, then the tip is moved one pixel in the y-direction to record a new line in the x-direction. Both datasets of the forward and backward traces are immediately displayed during the experiment and are stored for later analysis. The fast scan direction is realised by applying a voltage sequence with a triangular wave form to the x-piezo.

sition of one frame. Each such a frame consists of two images: a left-to-right and a right-to-left image. The data for those images are recorded during the forward and backward traces of the STM tip. In the configuration shown in Figure 10.4, the forward-backward direction (typically denoted by the ‘fast scan direction’) is the x-direction and the ‘slow scan direction’ corresponds to the y-direction. The fast scan direction is realised by applying a voltage sequence with a triangular wave form to the x-piezo.

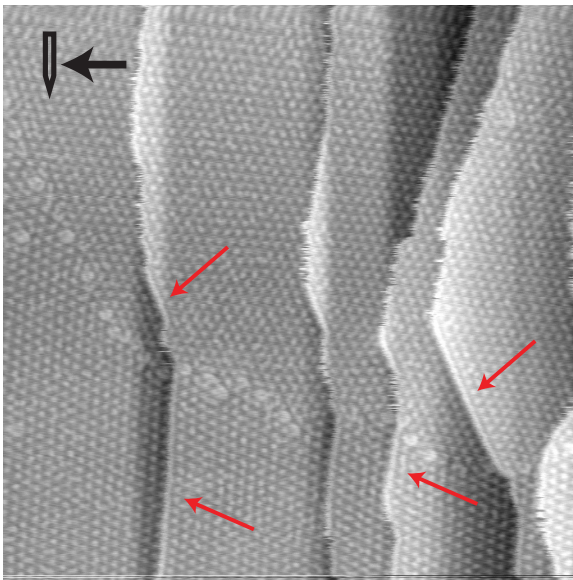
The timing of the STM was as such that the frequency of the triangular wave was 20 Hz. The pixel grid of the recorded image contained 1024×1024 pixels and the acquisition time of one frame was 51.2 sec. These timing settings mean that the time delay between two pixels placed next to each other in the slow scan direction is 50 ms in contrast to $24 \mu\text{s}$ in the fast scan direction.

10.3.2 Orientation dependence of fluctuations of buried iridium steps

A typical STM observation is shown in the two images presented in Figure 10.5. This data shows the same graphene covered iridium surface area, imaged with two different fast scan directions: bottom-to-top (Figure 10.5a) and right-to-left (Figure 10.5b). In these images, a line of defects is visible, which indicates the presence of a domain boundary between two differently oriented graphene domains. Also the moiré patterns indicate that the graphene domain at the top part of the image has a different orientation than



(a)



(b)

Figure 10.5: Two STM images of graphene on Ir(111) recorded successively at 1184K. In Figure (b), the red arrows highlight buried iridium steps that do not exhibit any mobility. The fast scan direction of the images is bottom-to-top for panel (a) and right-to-left for panel (b). Image size $117 \times 117 \text{ nm}^2$, z-scale 0.39 nm, sample voltage 4.5 V, tunnelling current 0.1 nA.

the graphene observed at the lower part of the image.

In both images presented in Figure 10.5 we can see that the mobility of the iridium steps underneath the graphene varies from one location to the other. Some parts of steps are affected by fluctuations, whereas other parts show up completely straight and static. When we compare Figures 10.5a and 10.5b, we see that straight, static parts of iridium steps show up similarly in both images. A few of these step sections are highlighted with red arrows in Figure 10.5b. In contrast, step sections that exhibit fluctuations in the upper panel, exhibit fluctuations in the lower panel as well. The different appearance of these fluctuations is discussed later in this section.

Here, we first focus on the distinction between the static, straight sections and the fluctuating parts of the buried iridium steps. As recognised before, we find that the straight step sections do not align with the lattice directions of the iridium substrate or the graphene overlayer. Instead, they follow directions of the moiré pattern. For all other orientations, the steps exhibit fluctuations. The large difference in fluctuation amplitude between the aligned and misaligned step sections can be understood easily. A misaligned step section necessarily contains macro-kinks, as can be seen in Figure 10.3. For such a step section to fluctuate, it only has to advance or recede the precise locations these existing macro-kinks. On the other hand, the only way for an aligned step section to fluctuate, is to first create new pairs of macro-kinks, which may be expected to require the investment of a sizeable formation energy.

The effect discussed here of the orientation of the buried step with respect to the moiré pattern comes in addition to the reduction in mobility that is introduced by the presence of the graphene overlayer. The latter reduction effect is clearly visible in Figure 10.1, which shows the large fluctuations of the free parts of the iridium step and the strongly reduced fluctuations of the buried step sections.

10.3.3 The ‘width’ of fluctuations

Figure 10.6 displays an STM image of a fluctuating iridium step underneath graphene, at a temperature of 1204 K. The red dashed lines in this figure are guides to the eye that are aligned to the moiré pattern, in order to indicate the size of the fluctuations. This analysis shows that the excursions the steps make in the direction perpendicular to the iridium step, have a typical size equal to size of the moiré unit cell. Again, we see that the influence of the moiré pattern on the behaviour of the iridium underneath the graphene is significant. Apparently, the local variations in interaction

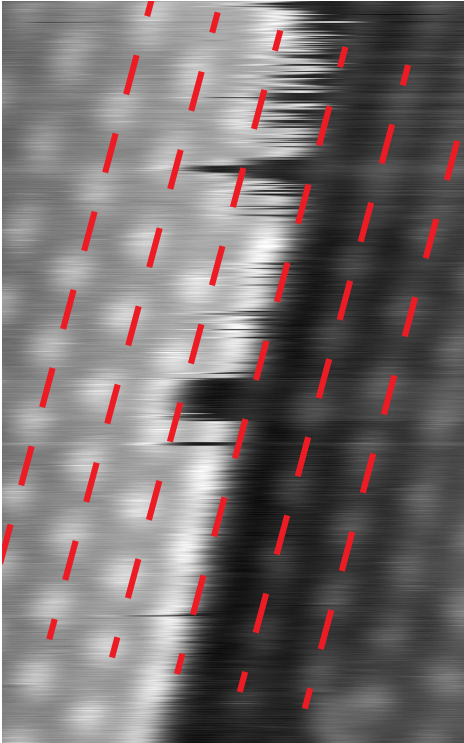


Figure 10.6: Fluctuations of an iridium step underneath graphene, observed by STM at a temperature of 1204 K. The red dashed lines run along the maxima of the moiré pattern (on the lower terrace). Image size $16 \times 26 \text{ nm}^2$, z-scale 0.17 nm, sample voltage 3.9 V, tunnelling current 0.1 nA.

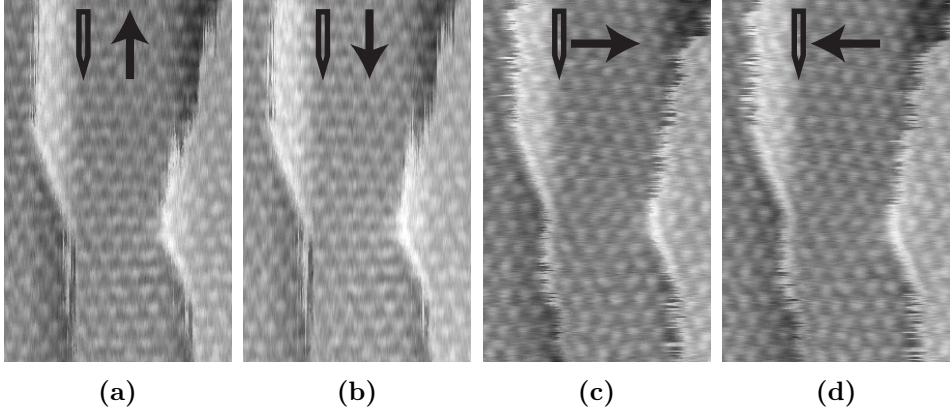


Figure 10.7: Four zoom-ins of STM observations at 1184K of two graphene-covered iridium steps, partially based on the images in Figure 10.5. The fast scan direction is indicated by the arrows. Panels (a) and (b) are composed of the forward (a) and backward (b) traces acquired nearly simultaneously on a subsection of the area also displayed in Figure 10.5a. Similarly, panels (c) and (d) are the forward and reverse traces, corresponding to the same section of Figure 10.5b. Taking into account the timing of the pixels, we see that the macro-kinks can travel readily over distances of 10 nm in 25 ms. Image size $27 \times 43 \text{ nm}^2$, z-scale 0.17 nm, sample voltage 4.5 V, tunnelling current 0.1 nA.

of graphene with the substrate make the iridium fluctuate in between the most stable states, which are a moiré lattice distance apart.

What Figure 10.6 also shows is that in addition to the large units of fluctuation, equal to the full size of a moiré unit cell, the iridium steps also perform rapid fluctuations with a small amplitude. This demonstrates that the preference is not absolute for the step to reside in the positions that are energetically optimal with respect to the moiré pattern; the step is seen to explore small excursions from the optimal positions that are dictated by the moiré pattern. We associate these more frequent, smaller-scale fluctuations with the more typical, atomic-scale step dynamics that is also responsible for the mobility of the uncovered parts of the step.

10.3.4 The ‘length’ of the fluctuations: rapid macro-kink motion

In Section 10.3.2 we have concluded from the orientation dependence of the mobility of graphene-covered steps that this mobility largely reflects

the random-walk motion of existing macro-kinks along the steps. In this section we will use the STM to inspect this motion more directly. Our first step is to compare the STM images in Figure 10.7. In these images, first the bottom-to-top and top-to-bottom traces of one recorded STM frame are shown. The right two panels show the observation made in the subsequently recorded frame. In that frame, the scan direction was rotated 90° , which effectively swaps the fast and slow scan directions. As the triangle frequency used for the fast scan direction was set to 20 Hz, the time between a forward and the subsequent backward trace is 25 ms, the acquisition time between two pixels next to each other in the slow scan direction is 50 ms and the acquisition time between two pixels next to each other in the fast scan direction is $24 \mu\text{s}$.

We first point out that in all four panels of Figure 10.7, two parts of the iridium steps do not exhibit any mobility. From this observation we can conclude that at the timescale of 50 sec (approximately the frame acquisition time) there is no mobility of these part of the iridium steps.

In Figures 10.7c and 10.7d, the mobile sections of the buried iridium steps show up very noisy. Although the noise in panels (c) and (d) is highly correlated, subtle differences can be distinguished already between the forward and reverse scan lines. Between subsequent scan lines within the same panel, the differences are already substantial and excursions over a distance of a full moiré unit can appear or disappear. From this we can conclude that the fluctuations over moiré-unit distances take place on a timescale less than 25 ms

Information on the magnitude, or ‘length’, of the fluctuations can be obtained from the observations shown panels (a) and (b) of Figure 10.7. In these images, the fluctuations appear different from those in panels (c) and (d): they show up as long stripes along the fast scan direction. The length of the stripes can be as large as 10 nm. Most of these stripes are connected at one side to the upper iridium terrace. This behaviour can only be explained by the mechanism in which only individual macro-kinks are moving along the step. The step motion is not caused by the creation of pairs of a macro-kink and an anti-macro-kink. The images in Figure 10.7 indicate that the diffusing macro-kinks can readily traverse distances of 10 nm in 25 ms.

For a macro-kink to move along the step over the minimum distance of a single moiré unit, 81 iridium atoms have to be relocated over significant distances, e.g. over the distance to the next kink[96]. The observed large fluctuations in macro-kink position, of e.g. 10 nm on the timescale of the scan lines of 25 ms, imply an impressive mobility of these iridium atoms

along the graphene-covered steps.

We notice that the fluctuation behaviour of the graphene-covered iridium steps at high temperature is very reminiscent of the fluctuations of steps reported previously for a variety of vicinal metal surfaces at much lower temperatures, such as Cu(1 1 1) and Au(110) [90, 94, 95]. In that work, the atomic-scale mechanisms underlying these fluctuations were derived from the scaling of the step's mean square displacement versus time. In the present study, we have not attempted to quantify the time exponent of the mean square displacement, because it was more difficult than in the clean-surface studies to identify a sufficiently large number of long, fully unpinned step sections and because the extremely high temperatures made it unpractical to reach the low drift rates, required for obtaining meaningful values for the time-dependent step displacements. However, we should expect that the intimate contact between the graphene overlayer and the iridium terraces effectively only leaves a narrow region at the step, where iridium atoms can be mobile. This means that even when iridium atoms on a clean surface would have the possibility to detach from the step and diffuse over the terraces, the presence of the graphene overlayer would force them to return more or less immediately to the step, which would render their diffusion effectively to a one-dimensional random walk along the steps. In such cases, the time exponent of the step fluctuations should naturally adopt a value of $1/4$ [97]. There has been discussion about the nature of short-time correlations in the step motion [94, 96]. The combination of scan directions, across and along the steps, illustrated in Figures 10.5 and 10.7, provides direct evidence for the interpretation advocated in Reference [96] that the short-time correlations originate from rapid back-and-forth motion of existing kinks (in this case macro-kinks) along the steps.

10.4 Summary

We have performed STM studies of the system of graphene on an Ir(111) surface at the high temperatures that are typical for CVD growth of graphene on this substrate. The observations shine new light on the behaviour of the graphene and iridium at temperatures above 1000 K. First, we observe how graphene grows into iridium terraces and we understand how it is forced to 'climb' upwards one iridium plane when the progressing graphene has pushed iridium steps into contact with each other. We find that the iridium steps leave no noticeable signature in the graphene overlayer, which means that the steps have no lasting impact on the graphene quality.

Second, we studied the behaviour of iridium steps underneath graphene.

Advancement of iridium terrace edges underneath graphene is observed during graphene growth. The iridium atoms that add to these buried steps originate from the iridium steps that are forced to recede by the advancing graphene edges. Our images suggest that these iridium atoms can easily slip under the graphene at locations where an edge of a graphene island is draped over an iridium step. The observed mobility revealed a dominating influence of the moiré pattern: the shapes of the mobile iridium steps underneath graphene are strongly dominated by the moiré lattice. This goes not only for the preferred orientations of the steps, but also for the preferred locations, which results in macro-kinks with a width of the full moiré unit cell.

In case an iridium step was not aligned with the moiré lattice, strong fluctuations of the step, underneath the graphene, were observed. Our STM images show that they are caused by the rapid motion along the steps of individual, pre-existing macro-kinks. The macro-kinks easily travel over 10 nm in 25 ms, which involves the relocation of hundreds of iridium atoms over several nanometers within milliseconds.

Our high-temperature STM observations have enabled us to acquire direct insight in the complex dynamics of the system of graphene on a metal substrate. These findings help us to develop new and improved recipes for the synthesis of high-quality graphene by chemical vapor deposition.